

Supporting information

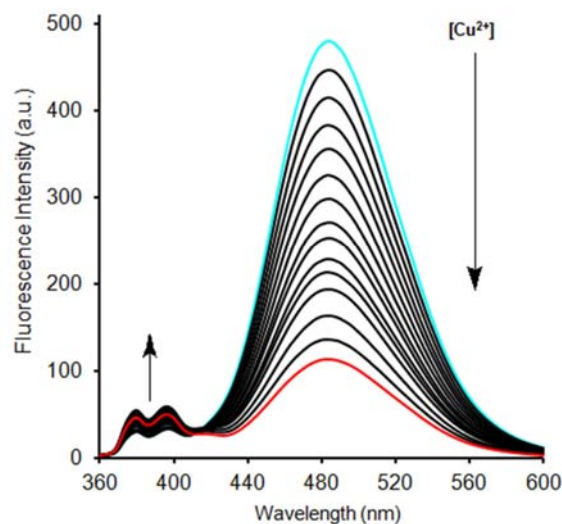


Figure S1. Fluorescence spectral of **L** (1.0 μM) upon addition of increasing concentrations of Cu²⁺ in CH₃CN / H₂O (v/v, 95:5) solution at 298K. $\lambda_{\text{ex}} = 343$ nm.

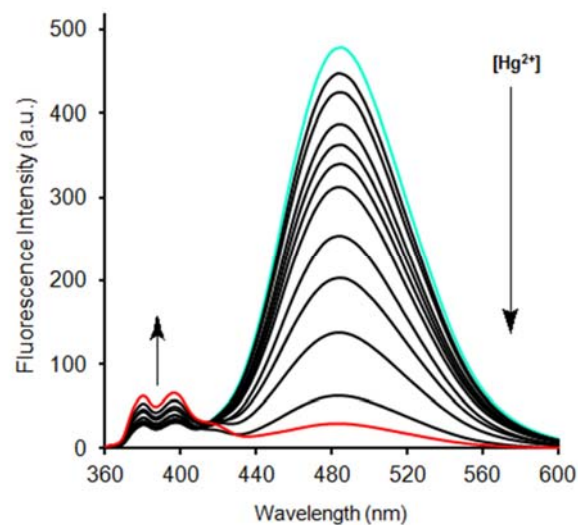


Figure S2. Fluorescence spectral of **L** (1.0 μM) upon addition of increasing concentrations of Hg²⁺ in CH₃CN / H₂O (v/v, 95:5) solution at 298K. $\lambda_{\text{ex}} = 343$ nm.

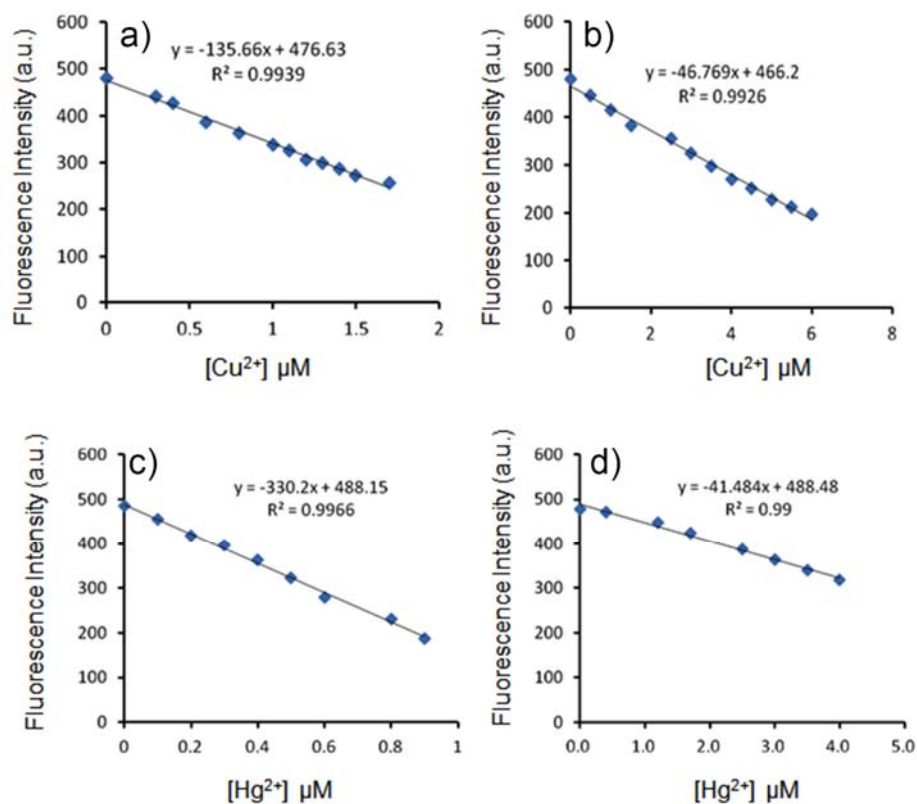


Figure S3. Plot of fluorescence intensity change (485 nm) of L with varied concentrations of Cu^{2+} and Hg^{2+} at 298K, the limit of detection of Cu^{2+} was calculated to be a) 4.54×10^{-9} M in CH_3CN , b) 1.87×10^{-8} M in $\text{CH}_3\text{CN}/\text{H}_2\text{O}$ (v/v, 95:5), and the limit of detection of Hg^{2+} was calculated to be c) 2.64×10^{-9} M in CH_3CN , d) 1.08×10^{-8} M in $\text{CH}_3\text{CN}/\text{H}_2\text{O}$ (v/v, 95:5), by the formula $(3\sigma/K)$.

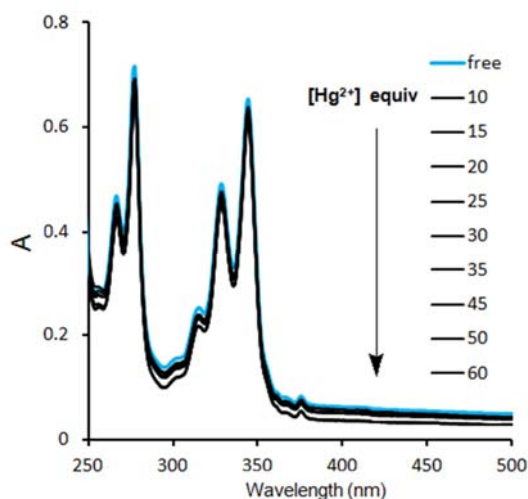


Figure S4. UV-vis spectral changes of L (1.0 μM) in $\text{CH}_3\text{CN} / \text{H}_2\text{O}$ solution (v/v, 95:5) with increasing concentration of Hg^{2+} ions.

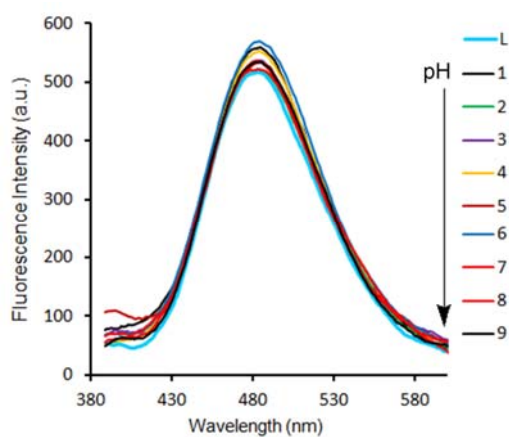


Figure S5. Fluorescence spectral changes of **L** ($1.0 \mu\text{M}$) in $\text{CH}_3\text{CN} / \text{H}_2\text{O}$ (v/v, 95:5) from pH 1.0 to 9.0. $\lambda_{\text{ex}} = 343 \text{ nm}$.

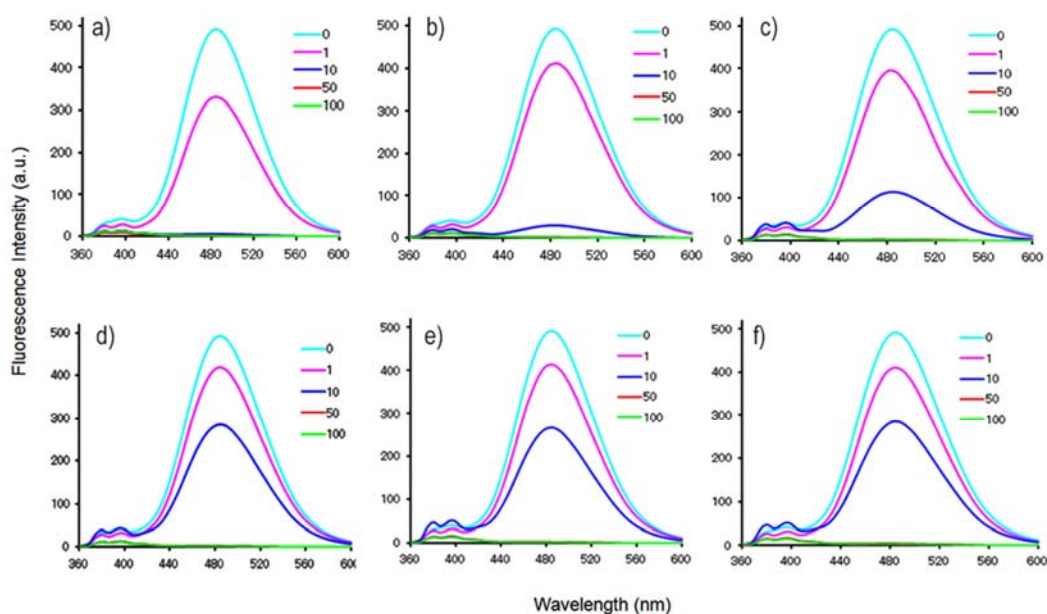


Figure S6. Fluorescence spectral changes of **L** ($1.0 \mu\text{M}$) upon addition of different concentrations of $\text{Hg}(\text{ClO}_4)_2$ (1, 10, 50, 100 μM) and determined immediately at 298 K in a) CH_3CN solution; b) 1% H_2O ($\text{H}_2\text{O}/\text{CH}_3\text{CN}$, v/v); c) 2% H_2O ($\text{H}_2\text{O}/\text{CH}_3\text{CN}$, v/v); d) 3% H_2O ($\text{H}_2\text{O}/\text{CH}_3\text{CN}$, v/v); e) 4% H_2O ($\text{H}_2\text{O}/\text{CH}_3\text{CN}$, v/v); f) 5% H_2O ($\text{H}_2\text{O}/\text{CH}_3\text{CN}$, v/v). $\lambda_{\text{ex}} = 343 \text{ nm}$.

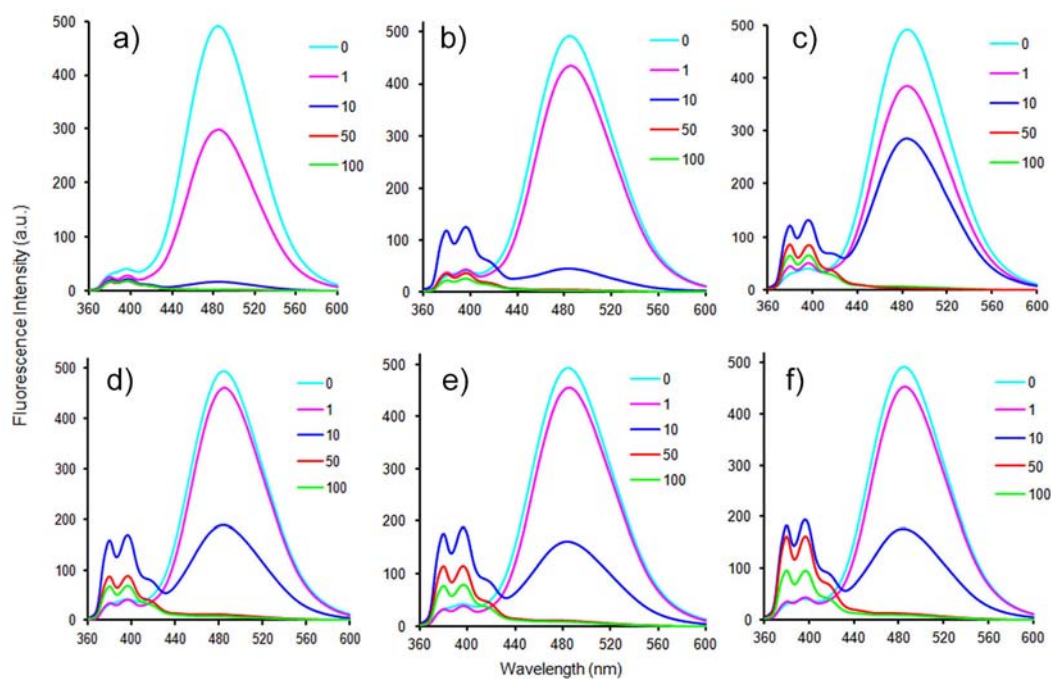


Figure S7. Fluorescence spectral changes of **L** (1.0 μM) upon addition of different concentrations of $\text{Hg}(\text{ClO}_4)_2$ (1, 10, 50, 100 μM) and determined after 48 h at 298 K in a) CH_3CN solution; b) 1% H_2O ($\text{H}_2\text{O}/\text{CH}_3\text{CN}$, v/v); c) 2% H_2O ($\text{H}_2\text{O}/\text{CH}_3\text{CN}$, v/v); d) 3% H_2O ($\text{H}_2\text{O}/\text{CH}_3\text{CN}$, v/v); e) 4% H_2O ($\text{H}_2\text{O}/\text{CH}_3\text{CN}$, v/v); f) 5% H_2O ($\text{H}_2\text{O}/\text{CH}_3\text{CN}$, v/v). $\lambda_{\text{ex}} = 343 \text{ nm}$.

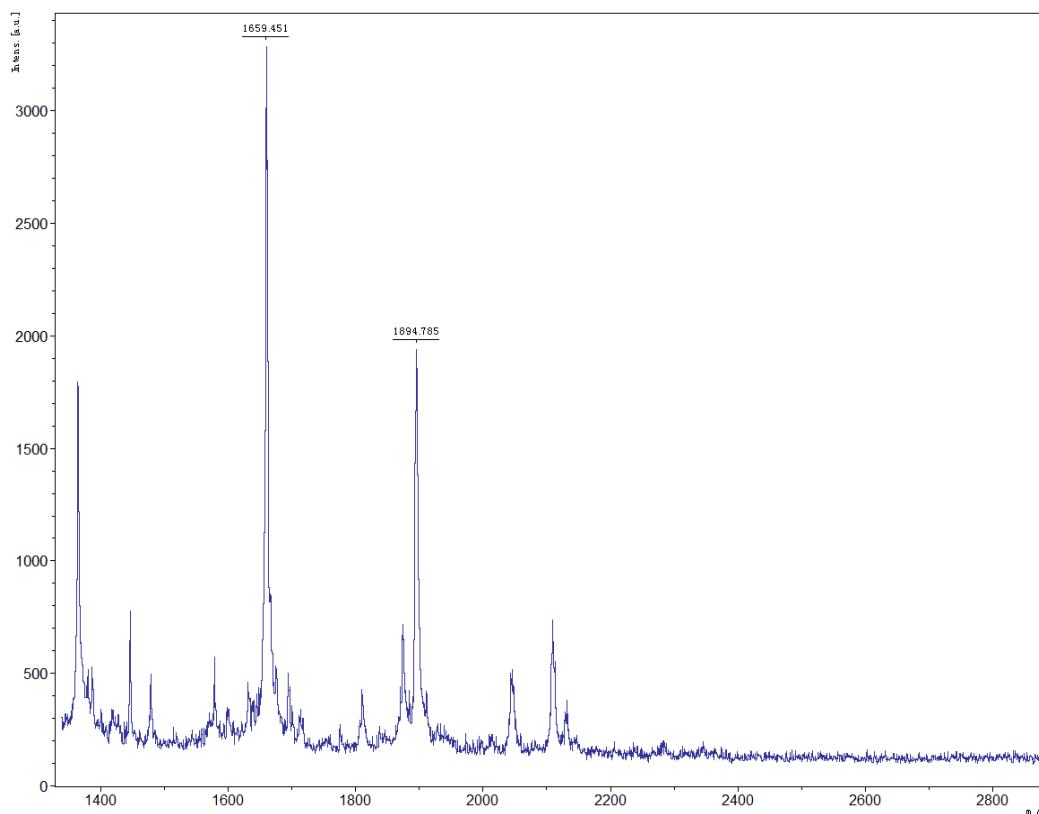


Figure S8. Matrix assisted laser desorption ionization time of flight mass spectrometry (MALDI-TOF) of **L**: $[\text{L} + \text{Hg}^{2+} + 3\text{H}_2\text{O} + \text{H}]^+$, m/z 1894.785.

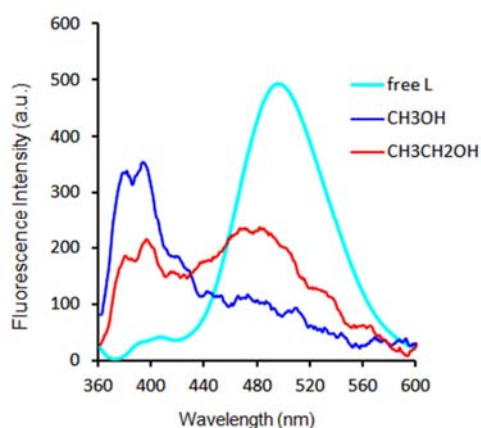


Figure S9. Fluorescence spectral changes of **L**-Hg²⁺ (**[L]**=1.0 μ M, **[L]**: [Hg²⁺]= 1:50) in CH₃CN solution upon addition 5% of CH₃OH, CH₃CH₂OH, respectively, and determined after 48 h.

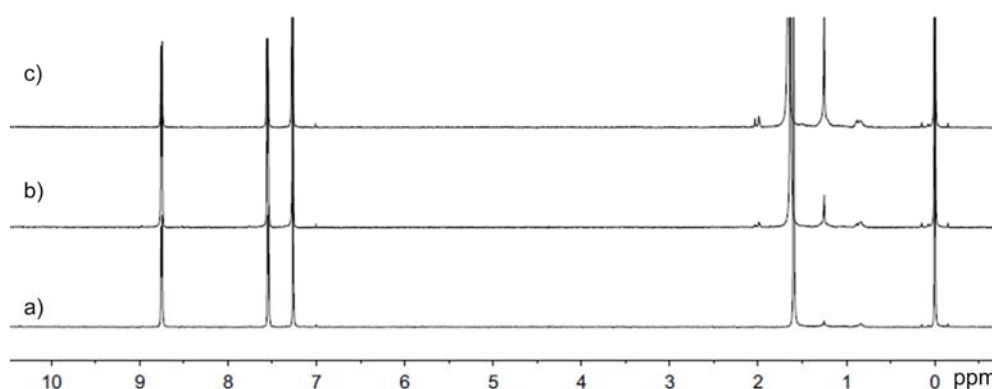


Figure S10. ¹H NMR spectral of 4,4'-bipyridine (3.0 mM) in the presence of different concentration of Hg(ClO₄)₂ a) free 4,4'-bipyridine, b) upon addition of 0.5 equiv of Hg(ClO₄)₂, c) upon addition of 1.0 equiv of Hg(ClO₄)₂ at 298 K.

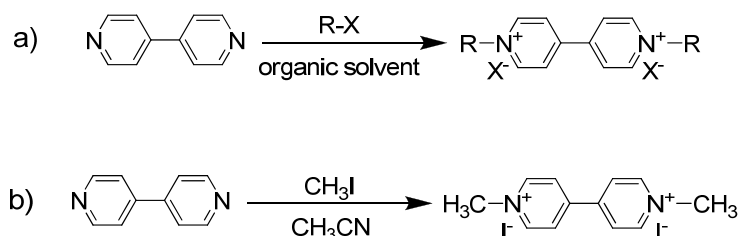


Figure S11. a) General chemical reaction based on 4,4'-bipyridine; b) representative of chemical reaction of 4,4'-bipyridine was selected in the present study.

Detail experiment procedure for reaction (b): CH₃I (284 mg, 2 mmol) was added to a 10 mL CH₃CN solution of 4,4'-bipyridine (156 mg, 1 mmol) and heated under 35 °C. During the reaction procedure, the reaction mixture was drawing 3 μ L by a syringe to 3 mL of **L**-Hg²⁺ solution (1.0 μ M of **L** with 50 equiv of Hg²⁺ in CH₃CN solution) in a cuvette after 1h, 2h, 3h, respectively, and then determined by fluorescence spectral immediately. The increasing monomer emission intensity of **L**-Hg²⁺ decreased with the reaction time increasing, which indicated that 4,4'-bipyridine was consumed dramatically after 3 h later (Figure S12).

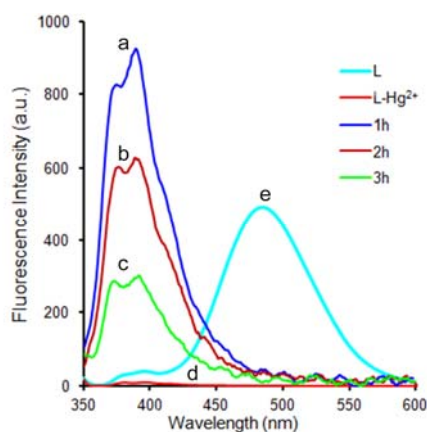


Figure S12. Fluorescence spectral changes of L-Hg^{2+} ($1.0 \mu\text{M}$ of L with 50 equiv of Hg^{2+} in CH_3CN solution) upon addition of the reaction mixture of 4,4'-bipyridine after a) 1h; b) 2h; c) 3h. at 298 K. $\lambda_{\text{ex}} = 343 \text{ nm}$.

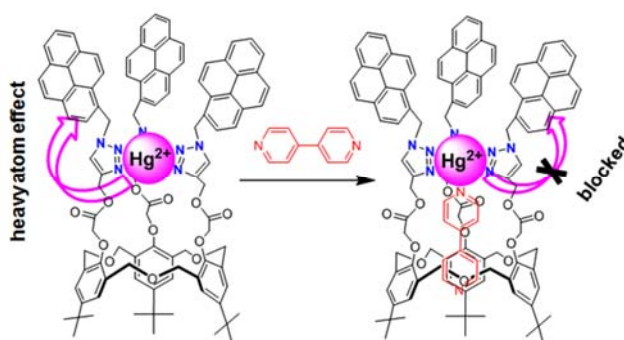


Figure S13. Plausible mechanism of heavy atom effect blocked by 4,4'-bipyridine in L-Hg^{2+} complex.

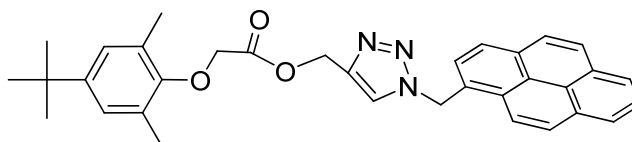


Figure S14. Molecular structure of **M**.

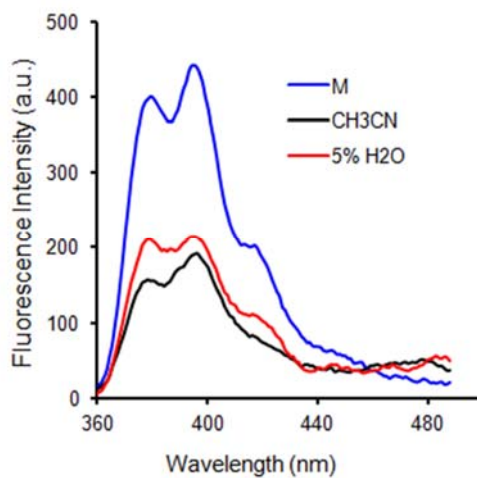


Figure S15. Fluorescence spectral changes of **M** ($1.0 \mu\text{M}$) upon addition of 50 equiv. of $\text{Hg}(\text{ClO}_4)_2$ in CH_3CN and $\text{H}_2\text{O}/\text{CH}_3\text{CN}$ (v/v, 5:95) solution, respectively at 298K, and determined immediately at 298 K. $\lambda_{\text{ex}} = 343 \text{ nm}$.

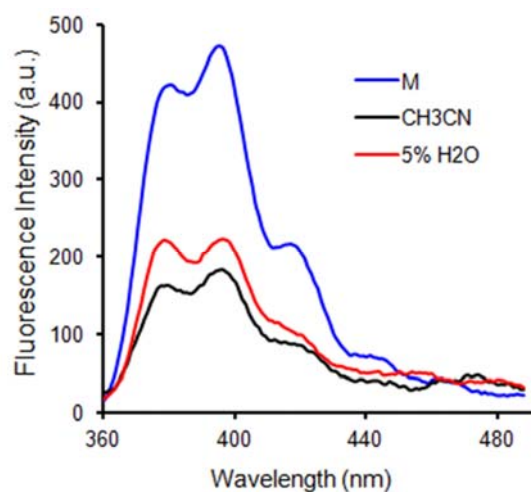


Figure S16. Fluorescence spectral changes of **M** ($1.0 \mu\text{M}$) upon addition of 50 equiv. of $\text{Hg}(\text{ClO}_4)_2$ in CH_3CN and $\text{H}_2\text{O}/\text{CH}_3\text{CN}$ (v/v, 5:95) solution, respectively at 298K, and determined after 48 h at 298 K. $\lambda_{\text{ex}} = 343 \text{ nm}$.

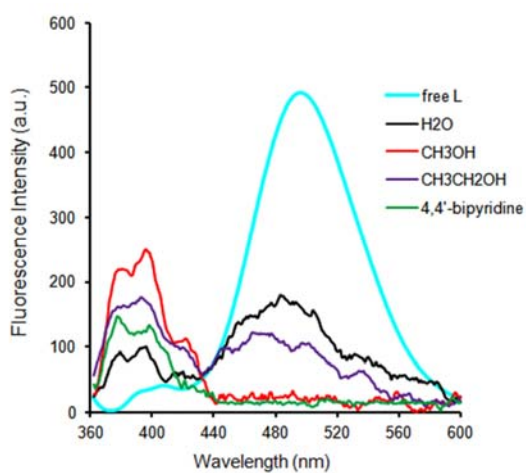


Figure S17. Fluorescence spectral changes of **L**- Cu^{2+} ($[\text{L}] = 1.0 \mu\text{M}$, $[\text{L}]: [\text{Cu}^{2+}] = 1:50$) in CH_3CN solution upon addition 5% of H_2O , CH_3OH , $\text{CH}_3\text{CH}_2\text{OH}$ and 20 equiv of 4,4'-bipyridine, respectively, and then determined after 48 h.